THE EUROPEAN
PHYSICAL JOURNAL C

CrossMark

Two scales in Bose–Einstein correlations

V. A. Khoze[1,2,a], **A. D. Martin**[1], **M. G. Ryskin**[1,2], **V. A. Schegelsky**[2]

[1] Institute for Particle Physics Phenomenology, University of Durham, Durham DH1 3LE, UK
[2] Petersburg Nuclear Physics Institute, NRC 'Kurchatov Institute', Gatchina, Saint Petersburg 188300, Russia

Abstract We argue that the secondaries produced in high-energy hadron collisions are emitted by small-size sources distributed over a much larger area in impact parameter space occupied by the interaction amplitude. That is, Bose–Einstein correlation of two emitted identical particles should be described by a 'two-radii' parametrisation ansatz. We discuss the expected energy, charged multiplicity and transverse momentum of the pair (that is, $\sqrt{s}$, N_{ch}, k_t) behaviour of both the small and the large size components.

1 Introduction

An effective tool to study the space-time structure of the production amplitude is to measure the Bose–Einstein correlations (BEC) between two identical particles produced in the inclusive hadron interaction; see, for example, [1–7]. Consider the situation where we have one pion with momentum p_1 emitted at point r_1 and another identical pion with p_2 and r_2. The inclusive cross section for the two identical particles takes the form

$$\frac{E_1 E_2 d^2\sigma}{d^3 p_1 d^3 p_2} = \frac{1}{2!} |M|^2 \langle 2 + 2 e^{irQ} \rangle = |M|^2 \langle 1 + e^{irQ} \rangle, \tag{1}$$

where M is the production amplitude, and where we have the 4-vectors $Q = p_2 - p_1$ and $r = r_1 - r_2$. The $\langle ... \rangle$ denote the averaging over r_1 and r_2. The e^{irQ} term is due to the permutation of the identical pions; that is, it allows for the pion with p_2 to be emitted from the point r_1 and simultaneously for p_1 from r_2. As a rule the Q dependence of the amplitude M is relatively flat in comparison with the Q dependence of e^{irQ}. Thus we are able to evaluate the size of the pion production domain by studying the Q dependence of the whole cross section $d^2\sigma$.

To extract the effect we compare the measured Q spectrum with a similar one but without BEC. To be precise we form the ratio

$$R(Q) = \frac{\mathrm{d}N/\mathrm{d}Q - \mathrm{d}N_{\mathrm{ref}}/\mathrm{d}Q}{\mathrm{d}N_{\mathrm{ref}}/\mathrm{d}Q} \tag{2}$$

where $\mathrm{d}N/\mathrm{d}Q$ is the two pion distribution integrated over all the variables except Q, and $\mathrm{d}N_{\mathrm{ref}}/\mathrm{d}Q$ is the distribution expected in a world without BEC. There are different ways to choose $\mathrm{d}N_{\mathrm{ref}}/\mathrm{d}Q$. We may measure the $\pi^+\pi^-$ distribution for non-identical pions; or we may change the sign of the three momentum of the second pion $\vec{p}_2 \to -\vec{p}_2$; and so on. None of these approaches compensates for the Q dependence of M completely; but for the conventional 'one-radius' fit

$$R(Q) = \lambda e^{-\bar{r}Q} \tag{3}$$

the different values of the mean radius,[1] $\bar{r}$, extracted from the data are close to each other. Such analyses of high-energy proton–proton interactions at the LHC have been performed by ATLAS [8], CMS [9] and ALICE [10]. For an analysis of lower energy data see, for example, the review in Ref. [7]

The problem is that the value of λ turns out to be less than 1. In particular, CMS claim $\lambda = 0.62 \pm 0.01$ [9]. On the other hand from (2) we expect $R(Q = 0) = 1$. Moreover, it is clear from Fig. 1 of [9], and the analogous plots of the other groups, that the fit does not describe the very low Q data points. This indicates that there should be another component of $R(Q)$ with a larger radius populating the region of small Q.

In the present paper we argue that the expected structure of the pion emission domain is highly inhomogeneous. We should consider *small* size pion sources distributed in the much larger area of the proton–proton interaction. That is, we are led to parametrise $R(Q)$ by two different mean radii. We explain the physical origin of this situation below.

---

a e-mail: v.a.khoze@durham.ac.uk

---

[1] The 'mean' radius, $\bar{r}$, is such that $e^{-\bar{r}Q}$ approximates the value of e^{irQ} averaged over r_1 and r_2.
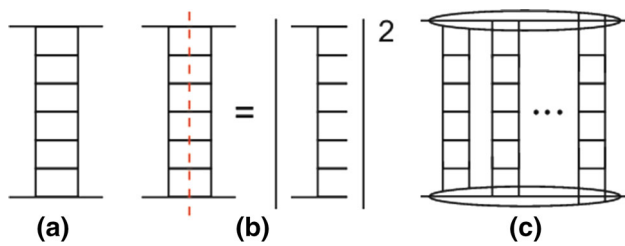
Fig. 1 **a** The ladder diagram for one-pomeron exchange, **b** cutting one-pomeron exchange leads to the multiperipheral chain of final state particles, **c** a multipomeron exchange diagram

2 Mechanisms for multiparticle production

It was shown long ago that to describe a high energy (say, proton–proton) interaction it is convenient to first select the subset of diagrams which provides the interaction across a large rapidity gap, and whose contribution does not decrease when the rapidity separation increases [11]. The resulting ladder-like set of diagrams forms Reggeon exchange. In terms of the hadronic degrees of freedom the corresponding subset of diagrams—called multiperipheral ladder diagrams (Fig. 1a)—was studied first by Amati et al. [12]. In terms of QCD[2] they form the BFKL pomeron [15]. In a general purpose Monte Carlo these are the diagrams for the DGLAP evolution amplitude. To be precise, in a Monte Carlo we do not simulate the elastic scattering amplitude, but rather the cross section of multiparticle production which can be viewed as the 'cut' of the amplitude shown in Fig. 1b. Besides one-ladder (one-pomeron) exchange there are more complicated multipomeron diagrams generated by unitarity [11], like those in Fig. 1c. In terms of the amplitude these diagrams describe the screening corrections to the one-pomeron contribution. If we simultaneously cut a few ladders (pomerons), say n_P, in such diagrams, then we obtain a cross section in which the density of the secondaries is n_P times larger than that produced by cutting a single ladder [16]. In a Monte Carlo this is called the Multiple Interaction (MI) option.[3]

Already at this stage we observe two quite different scales. The slope, $B_{\rm el}$, of elastic proton–proton scattering is usually parametrised in the form

$$B_{\rm el}(s) = B_0 + 2\alpha'_P \ln(s/s_0), \tag{4}$$

where the constant B_0 is driven by the size of an incoming proton. On the other hand, the value of α'_P reflects the internal transverse size of the ladder. Based on the pre-LHC data,

typical numbers are $B_0 \sim 10\,\mathrm{GeV}^{-2}$ and $\alpha'_P \sim 0.25\,\mathrm{GeV}^{-2}$ [17,18].

Strictly speaking, (4) corresponds to one-ladder exchange and not to the experimentally observed slope of the elastic cross section. The absorptive corrections described by the multi-ladder diagrams Fig. 1c speed up the shrinkage of the diffractive cone. Indeed, the screening is stronger in the centre of the disk (that is, at small impact parameters where the one-ladder contribution is larger) than at the periphery. Therefore the mean radius of the full amplitude becomes larger than that caused by one-pomeron exchange. Since the probability of interaction increases with energy at high energies this effect becomes more important and more visible.

Asymptotically, we reach the black disc limit, where the total cross section grows as $\ln^2 s$ and the slope $B_{\rm el}(s)$ also increases as $\ln^2 s$. It was shown [19] that indeed the high-energy LHC data indicate the presence of a $\ln^2 s$ component in the elastic slope which is consistent with the growth of the total cross section. Thus the radius of the whole amplitude slowly increases with energy. However, this is not true for the radius of an individual ladder. Within the old multiperipheral model(s), where the value of mean transverse momentum was limited, this radius (that is, the value of α'_P) does not depend on energy. On the other hand, QCD is a logarithmic theory and here the value of α'_P slowly decreases with energy due to the larger available k_t space. Indeed, it is well known that $\alpha'_P \to 0$ in the BFKL case.

Another example is the Monte Carlo description of multiparticle production. In order to tune the generator to describe the high-energy data one has to introduce an infrared cutoff, $k_t^{\min}$ whose value grows as $s^{0.12}$ [20]—that is, the transverse size of the ladder decreases. Recall that actually $k_t^{\min}$ acts as the cutoff in the 'hard' matrix element and not in the whole ladder. However, since the DGLAP ladder describes the evolution starting from some relatively large hadron size up to the scale (i.e. the inverse size) of the hard matrix element, the mean transverse momenta of secondaries produced by such a ladder also increases with the growth of the 'hard' scale driven by $k_t^{\min}(s)$. Thus the mean transverse size of the ladder decreases.

The resulting picture therefore looks as follows. The interaction of high-energy protons is described by diagrams like Fig. 1c in which the size of each individual ladder is rather small (as seen from the small value of α'_P). Yet the separation between the ladders is of the order of the radius of the interaction amplitude, which should be correlated with the total value of $B_{\rm el}(s)$. With increasing energy we expect the transverse size of an individual ladder (measured in the central rapidity interval) will decrease (as indicated by the behaviour of $k_t^{\min}(s)$). On the other hand the separation between the ladders is expected to increase, as indicated by the behaviour of $B_{\rm el}(s)$.

---

[2] For simple discussions of the transfer from hadronic to QCD ladders see the appendix of [13], and [14].

[3] For simplicity, we do not consider here the possibility of pomeron–pomeron interactions or the splitting of one ladder into two ladders (and/or the fusion of two ladders into one ladder). This does not change our qualitative conclusion, particularly as the corresponding couplings are rather small.

3 Two components in Bose–Einstein correlations

Having the above picture in mind, we expect in BEC to observe a new object—a small-size pion source. In other words, BEC should be described by two different radii.[4] One radius corresponds to the case when both pions are emitted from the same ladder—this will measure the size of an individual 'pomeron'. Since the pion is not a point-like object the radius will be smeared out by fluctuations in the process of the formation of the pions. The second radius will correspond to the pions being emitted from two different ladders—it is a measure of the separation between the ladders. Therefore we propose to fit the observed correlation $R(Q)$ by a formula with two different mean radii[5]

$$R(Q) = \lambda\, e^{-\bar{r}_1 Q} + (1-\lambda)\, e^{-\bar{r}_2 Q}, \qquad (5)$$

which better reflects the complicated structure of the pion emission domain. In the ideal case we expect the low multiplicity events to be produced via a diagram with only one 'cut' pomeron exchange (Fig. 1b). In general there may be more pomerons in the whole amplitude, but only one ladder radiates the secondaries. As the multiplicity becomes larger the secondaries are mainly emitted from a few different ladders, and the probability to find the two identical pions originating from the same pomeron decreases. That is, we expect the relative contribution λ of the large component (described by, say, $\bar{r}_1$) to increase with N_{ch}, while on the other hand, the strength of the small-size component $(1-\lambda)$ decreases. Unfortunately we cannot predict that $\lambda \to 0$ as $N_{ch} \to 0$, and that $\lambda \to 1$ for very large N_{ch}. The situation is complicated by the strong fluctuations of the number of sec-

---

[4] The fact that high-energy hadron interactions should be described by a few different radii is not new. In particular, in [21] it was shown that the component where two pions are radiated from two different ladders should be described by another radius than that for the case with two pions from the same ladder. Moreover, pions coming from the decay of a narrow resonance with small width, Γ_{tot}, will be produced at larger distances $\sim 1/\Gamma_{tot}$ and thus correspond to a larger radius. The role of multipomeron diagrams in long-range rapidity correlations was considered, for example, in [22] for high multiplicity events at CERN-ISR energies, while in [23,24] nuclear–nuclear collisions were discussed. It was shown that the transverse radius is driven by the radius of the smaller nucleus. On the other hand, the longitudinal radius is determined by the hadronic longitudinal size. The presence of two different radii and the fact that the size of the source of secondary gluons is much smaller than the proton radius was considered also in [25] for the case of pA collisions. However, until now no analysis of BEC with two different transverse radii was performed for high-energy proton–proton collisions. We hope that the very high statistics available at the LHC will allow a study BEC in relatively small bins of $\Delta N_{ch} \sim 10$–20 with pion mean transverse momenta of $\Delta k_t \sim 200$ MeV (see Sect. 4) so that we can observe the predicted effect.

[5] Instead of the linear exponents, as in (5), other parametric forms may be considered for each term. For example, the second term may be a Gaussian, $e^{-(\bar{r}_2 Q)^2}$. The choice should be based on statistical criteria or on the relative strength of the two terms.

ondaries in each ladder (or pomeron). Recall that actually we do not measure the total charged multiplicity of an event, but rather the number of secondaries in a limited central rapidity interval (like $|\eta| < 2.5$ in the case of ATLAS and CMS). Then the multiplicity corresponding to one pomeron is relatively small ($N_{ch} \sim 4$) and the fluctuations strongly wash out the relation between the measured values and the number of cut pomerons. Moreover, for very low N_{ch} we may sample contributions from diffractive dissociation which have a qualitatively different structure. Nevertheless at large N_{ch} the multipomeron contribution dominates; that is BEC are driven mainly by the component with the largest radius, $\bar{r}_1$. Indeed it is seen in Fig. 3b of [8] that, in the *one* radius fit, (3), the radius increases with multiplicity reaching *saturation* of $\bar{r} \simeq 2$ fm for $N_{ch} \gtrsim 50$.

Such saturation was predicted in [26], where it was explained that the radius measured in a one-radius fit, is driven, not by the initial energy, but mainly by the number of cut pomerons, $n_P \propto N_{ch}$.[6] Indeed, the radius of the individual pomeron depends weakly on energy ($\alpha'_P \simeq$ const.), while the number of cut pomerons observed in the event (that is the separated pion sources) is proportional to N_{ch}. So the probability to have two identical pions from two different sources increases with N_{ch}. When $n_p = 1$ (at low N_{ch}) we observe one pomeron and measure its radius. On the other hand, for large N_{ch} we study the separation between the pomerons and the value of $\bar{r}$ is saturated at the radius of the interaction amplitude $\bar{r} \propto \sqrt{B_{el}(s)}$. It was shown in [26] that $B_{el} \sim 20$ GeV^{-2} [29] corresponds in a 'one-radius' fit to $\bar{r} = 2.2$ fm, which is in good agreement with Fig. 3b of the ATLAS fit [8].

We emphasise that the separation between the pomerons (the pion sources) is not equal to the incoming hadron (proton) radius. First note, the radius corresponding to the interaction amplitude is larger. It increases with energy. Recall that in each successive step of the ladder in Fig. 1 the impact parameter changes by Δb_t. This leads to a diffusion in b_t, which results in the second (or α'_p) term in the equation for the elastic slope, (4). Next, the pion is not a point-like particle and its formation also occupies some volume. Finally, there may be an interaction between the final state secondaries.

Strictly speaking the picture that we describe above corresponds to the initial stage of the interaction, and does not allow for possible final state rescattering. If there are final state interactions (either in terms of a hadron gas or a quark–

---

[6] This behaviour was first observed by the UA1 group. It was shown in Fig. 4 of [27,28] that the radius and the 'incoherence parameter' λ (as measured by BEC in a one-scale Gaussian fit) did not depend on energy in the $\sqrt{s} = 200$–900 GeV interval within the error bars. Rather they depend strongly on the particle density, that is on the number of cut pomerons. Note also that the value of λ observed in this experiment was rather low, $\lambda = 0.15$–0.4, indicating the presence of a second component with another radius.

gluon plasma) then BEC will measure the radius given by the point of the last interaction—that is, the domain occupied by secondaries is extended up to the stage where the particle density becomes so low that further interaction is very unlikely, and the size of the domain at which the last interaction occurs will be seen in BEC. The probability of final state rescattering increases with particle density N_{ch}. If this contribution were to dominate, then it is natural to expect $\bar{r} \propto (N_{ch})^{1/3}$. However, the data of Fig. 3b of [8] do not show any evidence of such a behaviour for large N_{ch}.

So what are the expectations of the 'two-radii' fit? The contribution of a small radius dominates at low N_{ch} and decreases with increasing N_{ch} [26]. The value of the small radius, $\bar{r}_2$, is almost independent of energy—there is a small tendency to decrease due to a larger k_t in the ladder (see, for example [30]). On the other hand, the strength of the $\bar{r}_1$ component increases with N_{ch}—the value of the radius, $\bar{r}_1$, correlated with B_{el} (that is, the radius of interaction of the incoming protons) slowly increases with energy. At asymptotic energies we expect $B_{el} \propto \ln^2 s$. A tendency already seen in LHC data [19]. Therefore for $s \to \infty$ we expect $\bar{r}_1 \propto c \ln s$. However, the coefficient c is numerically quite small.

For very large N_{ch} the value or $\bar{r}_1$ may additionally increase due to the final state rescattering, as was discussed above. However, it is not seen in the 7 TeV pp collision data.

4 The k_t dependence of BEC

Here we discuss the dependence of the radii, $\bar{r}_1$, $\bar{r}_2$, on the transverse momentum of the identical pair, $k_t = (p_1 + p_2)_t /2$, First, we make a trivial remark—for larger k_t we have better space resolution in implementing the BEC method. At low k_t it may be hard to distinguish between $\bar{r}_1$ and $\bar{r}_2$ components, since the radii $\bar{r}_1$ and $\bar{r}_2$ will be larger than that measured at large k_t due to uncertainty principle smearing, and thus will be closer to each other.

Recall that the probability to produce two large k_t pions from different ladders (pomerons) decreases with increasing k_t as the single particle inclusive cross section decreases steeply with k_t. That is, two identical pions, each with large k_t, should be produced from the same large k_t jet. So with increasing k_t of the pair we expect a large contribution from the $\bar{r}_2$ component with the value of $\bar{r}_2$ decreasing, reaching saturation corresponding to the jet size. To be more precise, we mean the size of pion formation due to the hadronisation of large k_t jets. This tendency of $\bar{r}$ to decrease with increasing k_t was indeed observed in a 'one-radii' fit of LHC data; see Figs. 5 and 6 of [8]. However, the value of k_t was not sufficiently large to see saturation in these plots.

Another effect at very large k_t, which may give an important contribution to large N_{ch} events, concerns the multiplicity of jets which increase as $\exp(-c\sqrt{\ln E_T})$; see, for exam-

ple, [31,32]. However, the high E_T jet cross section is too small to identify this effect in the present data.

5 Conclusions

We emphasise that the dynamics of high-energy hadron interactions is based on subamplitudes of small transverse size which are distributed over the whole domain occupied by the full interaction amplitude. Thus, in BEC we have to observe a small-size object corresponding to the emission of both pions (or both kaons etc.) from a single subamplitude and a larger radius caused by events where the pions are produced from different subamplitudes. At large N_{ch} the relative contribution of the large radius component increases. Enlarging the k_t of the identical pion pair we improve the space resolution of the BEC analyser. This allows for a better separation of the contributions from the small and large radii components. When k_t becomes too large (say, $k_t \gtrsim 1$ GeV) the probability to produce such large k_t pions from two different subamplitudes becomes small. In this case BEC measures the radius of the 'jet' which emits this high k_t pair of identical pions. That is, we expect the radius to decrease with increasing k_t, reaching *saturation* for $k_t \gtrsim 1$ GeV.

References

1. R. Hanbury-Brown, R.W. Twiss, Phil. Mag. **45**, 663 (1954)
2. R. Hanbury-Brown, R.W. Twiss, Proc. Roy. Soc. **242A**, 300 (1957)
3. R. Hanbury-Brown, R.W. Twiss, Proc. Roy. Soc. **243A**, 291 (1957)
4. G. Goldhaber, W.B. Fowler, S. Goldhaber et al., Phys. Rev. Lett. **3**, 181 (1959)
5. G.I. Kopylov, M.I. Podgoretskii, Sov. J. Nucl. Phys. **15**, 219 (1972)
6. G.I. Kopylov, M.I. Podgoretskii, Sov. J. Nucl. Phys. **18**, 336 (1973)
7. G. Alexander, Rep. Prog. Phys. **66**, 481 (2003)
8. ATLAS Collaboration, G. Aad et al., Eur. Phys. J. C75 (2015) 466
9. CMS Collaboration, V. Khachatryan et al., JHEP **1105**, 029 (2011)
10. ALICE Collaboration, K. Aamodiet et al., Phys. Rev. D 84 (2011) 112004
11. V. N. Gribov, Sov. Phys. JETP 26 (1968) 414 [Zh. Eksp. Teor. Fiz. **53** (1967) 654]
12. D. Amati, A. Stanghellini, S. Fubini, Nuovo Cim. **26**, 896 (1962)
13. V.A. Khoze, A.D. Martin and M.G. Ryskin, Int. J. Mod. Phys. A 30 (2015) 08, 1542004 [arXiv:1402.2778 [hep-ph]]
14. V.A. Khoze, A.D. Martin, M.G. Ryskin, A.G. Shuvaev, J. Phys. **G36**, 093001 (2009)

15. B. L. Ioffe, V. S. Fadin and L. N. Lipatov, "Quantum chromodynamics: Perturbative and nonperturbative aspects," (Cambridge, UK: Univ. Pr. (2014) 585 p)
16. V. Abramovsky, V.N. Gribov, O.V. Kancheli, Sov. J. Nucl. Phys. **18**, 308 (1964)
17. A. Donnachie, P.V. Landshoff, Nucl. Phys. B **231**, 231 (1984)
18. A. Donnachie, P.V. Landshoff, Nucl. Phys. B **244**, 322 (1984)
19. V.A. Schegelsky, M.G. Ryskin, Phys. Rev. D **85**, 094024 (2012). [arXiv:1112.3243 [hep-ph]]
20. T. Sjostrand, S. Mrenna, P.Z. Skands, Comput. Phys. Commun. **178**, 852 (2008). [arXiv:0710.3820 [hep-ph]]
21. E.M. Levin, M.G. Ryskin, S.I. Troyan, Sov. J. Nucl. Phys. **23**, 222 (1976)
22. A. Capella, A. Krzywicki, Phys. Rev. D **18**, 4120 (1978)
23. A. Capella, A. Krzywicki, Z. Phys. C **41**, 659 (1989)
24. A. Capella, A. Krzywicki, E.M. Levin, Phys. Rev. D **44**, 704 (1991)
25. T. Altinoluk, N. Armesto, G. Beuf, A. Kovner, M. Lublinsky, Phys. Lett. B **752**, 113 (2016)
26. V.A. Schegelsky, A.D. Martin, M.G. Ryskin, V.A. Khoze, Phys. Lett. B **703**, 288 (2011). [arXiv:1101.5520 [hep-ph]]
27. UA1 Collaboration, C. Albajar et al. Phys. Lett. **B226**, 410 (1989)
28. UA1 Collaboration, C. Albajar et al. Phys. Lett. **B229**, 439 (1989)
29. G. Antchev et al., TOTEM Collaboration. Europhys. Lett. **101**, 21002 (2013)
30. V.A. Khoze, A.D. Martin, M.G. Ryskin, Eur. Phys. J. C **74**, 3199 (2014). [arXiv:1409.8451 [hep-ph]]
31. L.V. Gribov, E.M. Levin, M.G. Ryskin, Phys. Rept. **100**, 1 (1983)
32. V.A. Khoze, W. Ochs, Int. J. Mod. Phys. A **12**, 2949 (1997). [hep-ph/9701421]